

## Bearing Failure Optimization of Composite Double-Lap Bolted Joints Based on a Three-Step Strategy Marked By Feasible Region Reduction and Model Decoupling

Fengrui Liu<sup>1,2,3</sup>, Wanting Yao<sup>1,2</sup>, Xinhong Shi<sup>4,\*</sup>, Libin Zhao<sup>1,2</sup> and Jianyu Zhang<sup>5,\*</sup>

**Abstract:** To minimize the mass and increase the bearing failure load of composite double-lap bolted joints, a three-step optimization strategy including feasible region reduction, optimization model decoupling and optimization was presented. In feasible region reduction, the dimensions of the feasible design region were reduced by selecting dominant design variables from numerous multilevel parameters by sensitivity analyses, and the feasible regions of variables were reduced by influence mechanism analyses. In model decoupling, the optimization model with a large number of variables was divided into various sub-models with fewer variables by variance analysis. In the third step, the optimization sub-models were solved one by one using a genetic algorithm, and the modified characteristic curve method was adopted as the failure prediction method. Based on the proposed optimization method, optimization of a double-lap single-bolt joint was performed using the ANSYS® code. The results show that the bearing failure load increased by 13.5% and that the mass decreased by 8.7% compared with those of the initial design of the joint, which validated the effectiveness of the three-step optimization strategy.

**Keywords:** Composite, bolted joints, sensitivity analysis, optimization.

### 1 Introduction

Advanced composites play important roles in aircraft structures because of their high strength/stiffness-to-weight ratios and the weight-saving requirements in the aerospace industry [Kumar and Srinivas (2018); Xu, Yang, Zeng et al. (2016); Zhang, Li, Wang et al. (2015); Sane, Padole and Uddanwadiker (2018)]. However, joints are commonly regarded as weak parts of composite structures because of the significant concentration of stress around bolt holes [Zhao, Yang, Cao et al. (2018); Zhao, Qin, Zhang et al. (2015); Liu, Lu,

---

<sup>1</sup> School of Astronautics, Beihang University, Beijing, 100191, China.

<sup>2</sup> Key Laboratory of Spacecraft Design Optimization and Dynamic Simulation Technologies, Ministry of Education, Beihang University, Beijing, 100191, China.

<sup>3</sup> State Key Laboratory for Strength and Vibration of Mechanical Structures, Xi'an Jiaotong University, Xi'an, 710049, China.

<sup>4</sup> Institute of Solid Mechanics, Beihang University, Beijing, 100191, China.

<sup>5</sup> College of Aerospace Engineering, Chongqing University, Chongqing, 400044, China.

\* Corresponding Authors: Xinhong Shi. Email: shixinhong@buaa.edu.cn.

Jianyu Zhang. Email: jyzhang@cqu.edu.cn.

Zhao et al. (2018)]. In composite bolted joint design, increasing the load carrying capacity and minimizing joint mass have become crucial but challenging issues in the efficient use of composites. The load carrying capacity and joint mass are influenced by numerous multilevel parameters. Therefore, it is necessary to develop an efficient design approach to seek the best performance of composite bolted joints in engineering.

To achieve a better structural performance and lower structural mass, various investigations have focused on the optimization of composite structures [Wu and Burgueño (2006); Lindgaard and Lund (2010); He and Aref (2003); Pelletier and Vel (2006); Manh and Lee (2014); Coelho, Guedes and Rodrigues (2015); Bakar, Kramer, Bordas et al. (2013); Kradinov, Madenci and Ambur (2007); Li, Huong, Crosky et al. (2009)]. Wu et al. [Wu and Burgueño (2006)] proposed an integrated approach for finding the optimal free-form three-dimensional shape and laminate stacking sequence design of fiber reinforced polymer shells. Lindgaard et al. [Lindgaard and Lund (2010)] proposed an approach for optimizing the nonlinear buckling fiber angle of laminated composite shell structures. He et al. [He and Aref (2003)] used a genetic algorithm to find the optimum design parameters of a fiber reinforced composite bridge deck, which included the number of stiffeners, the thickness and the orientations of outer skin layers. Pelletier et al. [Pelletier and Vel (2006)] presented a multi-objective optimization method for composite laminates based on an integer-coded genetic algorithm. The fiber orientations and volume fractions of the lamina were chosen as the primary optimization variables. Manh et al. [Manh and Lee (2014)] proposed an optimization model for aligning fibers in imperfect laminates based on a genetic algorithm and NURBS-based finite element isogeometric analysis. In addition to macroscopic parameters, such as the geometry configuration and stacking sequence, the mechanical performance of composite structures is also influenced by microscopic parameters. Coelho et al. [Coelho, Guedes and Rodrigues (2015)] used a multiscale topology optimization model to optimize bi-material composite laminates in which the fiber cross-section was designed to obtain the optimal microstructure. Bakar et al. [Bakar, Kramer, Bordas et al. (2013)] presented a genetic algorithm to optimize the elastic properties of woven fabric composites. The design variables included the gap length, yarn thickness, material constituents and effect of the shape factor.

Compared with the above simple laminates, only a few investigations have focused on the optimization of composite bolted joints. Based on a genetic algorithm and stress analyses, Kradinov et al. [Kradinov, Madenci and Ambur (2007)] achieved an optimum design of bolted composite joints. They considered the laminate thickness, lay-up, bolt locations, bolt flexibility and bolt sizes as design variables. Li et al. [Li, Huong, Crosky et al. (2009)] improved the bearing performance of composite bolted joints with reinforced z-pins. The volume contents and sizes of fibrous z-pins around the bolt holes were adopted as design variables. Clearly, recent investigations have generally focused on some of the design parameters of joints at the single scale, which has apparently restricted further exploration of the potential of composites.

The performance of composite bolted joints is influenced by numerous parameters [Saleeb, Wilt, Al-Zoubi et al. (2003); Friedrich, Wu, Thostenson et al. (2011); Zhang, Zhou, Chen et al. (2016)], including dimension parameters, assembling parameters,

unidirectional lamina, and the fiber and matrix, and an ideal optimization model involving all the relevant parameters for composite bolted joints is needed. In addition, an optimization strategy with high calculation efficiency is essential in engineering. Therefore, in this paper, an ideal optimization model for composite bolted joints that includes all the mechanical and geometric parameters is presented. Then, a three-step optimization strategy, including feasible region reduction, optimization model decoupling, and optimization based on the modified characteristic curve method, is presented. Finally, optimization of a single-bolt, double-lap joint is conducted to validate the effectiveness of the proposed ideal optimization model and three-step optimization strategy.

**2 Ideal optimization model for composite bolted joints**

A typical composite single-bolt double-lap joint is shown in Fig. 1. This figure shows a general multi-level framework of composite structures: from the microscopic fiber/matrix to the mesoscopic unidirectional lamina, macroscopic laminates and structure. An optimization model of composite bolted joints involving all the relevant parameters is an ideal model, which is the precondition for obtaining the optimal design of joints.

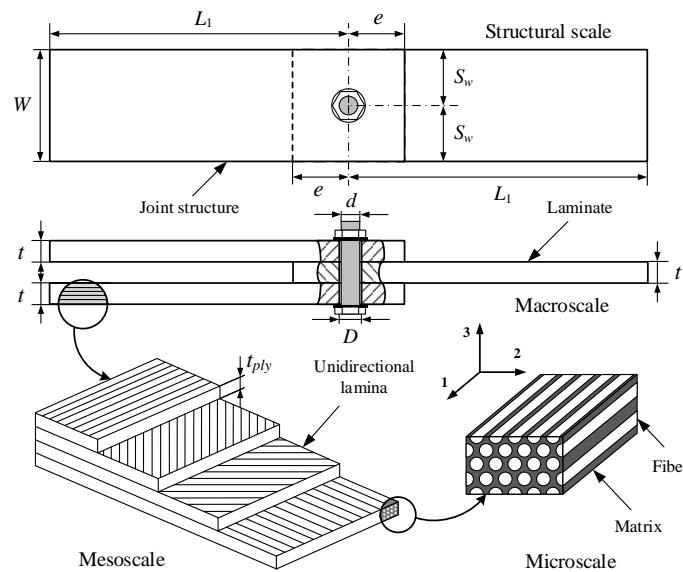


**Figure 1:** Multi-level description of a composite single-bolt double-lap joint

The three levels of parameters that affect the failure performance and mass of composite bolted joints were teased out and are listed in Tab. 1. The macroscopic geometry variables include dimension parameters and assembling parameters, which can directly impact the ultimate failure load, failure mode and structural mass. The majority of the mesoscopic parameters are unidirectional lamina properties, which affect the structural mass and failure load. The microscopic parameters are fiber/matrix constituent properties, which have a small effect on the structural mass but a more significant effect on the failure load.

**Table 1:** Multi-level variables of single-bolt double-lap joints

Parameter level	Parameters	Expression	
Macroscopic (Laminate)	Diameter of hole	$D$	
	Dimension parameters	Thickness	$t=n \times t_{ply}$
		End distance	$e$
		Width distance	$W=2S_w$
	Assembling parameters	Fit clearance	$\eta=D-d$
		Tightening torque	$N$
Friction coefficient		$\mu$	
Mesoscopic (Unidirectional lamina)	Number of unidirectional layers	$n$	
	Elasticity moduli	$E_{11}, E_{22}, E_{33}$	
	Shear moduli	$G_{12}, G_{13}, G_{23}$	
	Poisson ratios	$\nu_{12}, \nu_{13}, \nu_{23}$	
	Strength parameters of materials	$X_T, X_C, Y_T, Y_C,$ $S_{12}, S_{13}, S_{23}$	
	Thickness of unidirectional lamina	$t_{ply}=t/n$	
	Stacking sequence	$[\theta_1/\theta_2/\dots/\theta_n]$	
Microscopic (Fiber & Matrix)	Elasticity, shear modulus and Poisson ratio of fiber	$E_f, G_f, \nu_f$	
	Elasticity, shear modulus and Poisson ratio of matrix	$E_m, G_m, \nu_m$	
	Fiber and matrix volume fractions	$V_f, V_m$	

In Tab. 1, the subscripts 1, 2 and 3 are defined with the material principal coordinate systems, as shown in Fig. 1.  $X$  and  $Y$  represent the longitudinal and transverse strength properties of the unidirectional lamina, respectively, and  $S$  refers to the shear strength of the materials. The subscripts  $T$  and  $C$  represent the tensile and compressive strengths, respectively. At the microscale, the fiber and matrix are regarded as isotropic materials.

For the composite joint,  $D$ ,  $e$ ,  $S_w$  and  $t$  are decisive variables for the mass, and the mass can be mathematically expressed as follows:

$$m = 3\rho[2S_w(L_1 + e) - \frac{\pi D^2}{4}] \times t \quad (1)$$

where  $\rho$  is the average density of the composite material. Obviously,  $m$  increases with the increase of the macroscopic dimension factors  $e$ ,  $S_w$  and  $t$  of the laminate.

The objective of optimization in the present work is to simultaneously maximize the bearing failure load and minimize the joint mass. Adopting the method of division, the ideal optimization model of composite single-bolt double-lap joints can be expressed as:



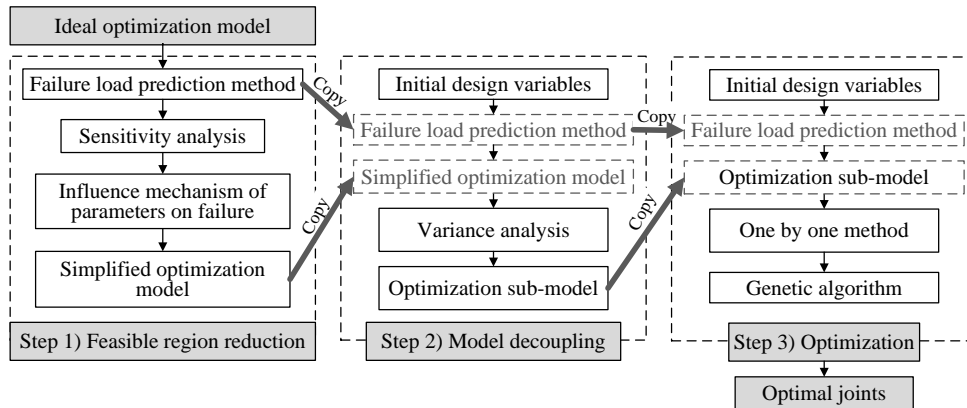


**Figure 2:** Flow chart of the optimization of composite bolted joints

The characteristics of the three-step optimization strategy include (1) sensitivity analyses coupled with influence mechanism analyses are conducted to reduce the feasible design region. Reduction of the feasible design region and computational complexity is achieved in two ways; (2) the original optimization model is decoupled into several sub-models to decrease the amount of calculations, which is an innovative idea. This idea works because the parameters of the joints are multi-level and easy to decouple; (3) the modified characteristic curve method, which is accurate and computationally efficient, is applied. The details of the optimization process of the ideal optimization model for composite bolted joints will be introduced in the following sections.

**3.2 Modified characteristic curve method for failure load prediction**

The large computation cost restricts the application of the progressive damage method (PDM) [Qin, Zhao, Xu et al. (2019)] for the optimization of composite structures, which is the most commonly used failure load prediction method for complex composite structures. Meanwhile, the characteristic curve method is suitable for predicting the failure load of composite bolted joints and attracts attention in engineering because of its simplicity and low computation cost as well as its good ability to accurately predict the failure load and failure mode.

In the current work, a modified characteristic curve method constructed by Zhang et al. [Zhang, Liu, Zhao et al. (2014)] was adopted to predict the failure loads and failure modes of composite bolted joints for subsequent sensitivity analysis, variables decoupling and optimization solving. Joint failure was detected when the stresses in any ply satisfies the modified Yamada-Sun failure criterion at any point on the characteristic curve. The modified characteristic curve, as shown in Fig. 3, is expressed as follows:

$$r = R + R_t + (R_c - R_t) \cos \theta + 2\alpha |\sin \theta| \cos \theta \quad -90^\circ \leq \theta \leq 90^\circ \tag{3}$$

where

$$\alpha = \frac{\sqrt{R_s^2 + R^2} [R_s^2 + R^2 - (R + R_t) \sqrt{R_s^2 + R^2} - R_s R_c + R_s R_t]}{2 R R_s} \tag{4}$$

and  $r$  is the distance from the center of the hole to any point on the modified characteristic curve;  $R$  is the diameter of the hole;  $R_t$ ,  $R_c$  and  $R_s$  are the tensile, compressive and shear-out characteristic lengths, respectively; and  $\theta$  is anticlockwise measured from the symmetry axis, which ranges in the interval of  $[-90^\circ, 90^\circ]$ . Tensile failure occurs when the failure point is located at  $75^\circ \leq |\theta| \leq 90^\circ$ ; bearing failure emerges at the region of  $0^\circ \leq |\theta| \leq 15^\circ$ , and shear-out failure occurs at  $30^\circ \leq |\theta| \leq 60^\circ$ . The composite material system and joint configuration used by Zhang et al. [Zhang, Liu, Zhao et al. (2014)] is the same as the composite bolt joint in the current work. Therefore, this method and the corresponding characteristic coefficients are applied to the failure prediction in the present work.

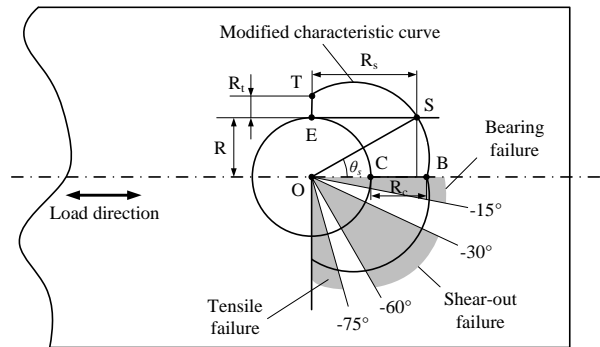


Figure 3: Modified characteristic curve method

### 3.3 Reducing the feasible design region to simplify the optimization model

#### 3.3.1 Selection of dominant variables based on sensitivity analysis

Multi-level parameters have different influences on the ultimate failure load of composite bolted joints. To reasonably choose the dominant design variables, sensitivity analysis [Camanho, Bowron and Matthews (1998); Li, Gu and Zhao (2017)] was applied to establish a ranking of the various parameters according to the influences of the parameters on the failure load.

Because only four parameters ( $D$ ,  $e$ ,  $S_w$  and  $t$ ) are related to joint mass, the sensitivity of other parameters to the joint mass  $m$  will give results of zero, and the sensitivity of other parameters to the load transfer efficiency  $f$  is only related to their sensitivity to the failure load. Therefore, the failure load  $F$  instead of the load transfer efficiency  $f$  is the objective of the sensitivity analysis, and  $D$ ,  $e$ ,  $S_w$  and  $t$  are considered to be dominant design variables. In the sensitivity analysis, other dominant design variables are selected from other multi-level parameters  $x_i$  ( $i=1, 2, \dots, n$ ), where  $n$  is the number of parameters. The sensitivity analysis can be expressed by the following formula, which represents the change of the failure load per unit of relative variation of the parameters.

$$S_i \approx \frac{\Delta F}{\Delta x_i / x_i} = \frac{F(x_1, x_2, \dots, x_i + \Delta x_i, \dots, x_k) - F(x_1, x_2, \dots, x_k)}{\Delta x_i / x_i} \quad (5)$$

where  $\Delta x_i$  refers to the variation of parameter  $x_i$ . Each  $\Delta x_i$  is determined by the standard deviation  $\sigma$  of the factor  $x_i$ , which is referenced to the maximum deviation of each parameter specified in the ASTM D5961 standard [ASTM D 5961 (2013)]. Considering the different units of the parameters, a relative non-dimensional increment form  $\Delta x_i / x_i$  was used in the sensitivity analysis to make the object evaluation comparable and fair.

### *3.3.2 Feasible region reduction of dominant variables based on the influence mechanisms*

The dimensions of the feasible design region decrease with the decrease in the number of optimization variables, and thus, the amount of optimization calculations decreases. Another way to reduce the feasible design region is to reduce the feasible region of the dominant variables, which also reduces the computational cost. This paper introduces influence mechanisms of variables that affect the failure behavior to further reduce the feasible design region. This analysis of influence mechanisms involves three aspects: fiber orientation, geometry parameters and tightening torque. Each analysis yields feasible regions of some dominant variables, and finally, a simplified optimization model with various dominant variables for composite bolted joints is obtained.

### *3.4 Model decoupling based on variance analysis*

There is still a high amount of computation in the optimization of the composite bolted joint because the number of dominant variables is large. As is known, the computation cost of an optimization model with  $n$  variables is much higher than that of the sum of  $n$  optimization models with one variable. To reduce the computational complexity, variance analysis is performed to study the interaction of variables. If the interaction term is not significant, a multivariate optimization can be decomposed into several optimizations with fewer variables or a single variable. Specifically, when the number of variables is known as  $n$ , the interaction term of any two variables is regarded as a factor and the quadratic term of the variables is taken into consideration; then, the total number of factors is  $2n+n(n-1)/2$ . The experiments of the  $2n+n(n-1)/2$  factors are arranged with an orthogonal table, and the level number of each factor is chosen according to the amount of calculations, such as 3. After the failure load of each test is obtained by using the failure prediction method presented in Section 3.2.1, variance analysis is carried out to determine whether the influence of the interaction term is significant. If the  $n-1$  interaction terms between a variable and other variables have little influence, the variable can be separately optimized, assuming that there are  $j$  variables in this case; if the interaction terms between  $m_i$  variables and the other  $n-m_i$  variables are not crucial, an optimization model with  $m_i$  variables can be separated, assuming the number of optimization models in this case is  $k$  and  $i=1\dots k$ . Apparently,  $n=j+m_1+\dots+m_k$ . Finally, the original optimization model is decoupled into  $j+k$  sub-models, and each sub-model has fewer variables than the original one.

### *3.5 Conducting optimization with the one by one method*

The sub-models will be solved one by one after the optimization model is decoupled, and then, the optimization results converge to a global optimal result. When a sub-model is

executed, the variables in the other optimizations remain constant, which substantially reduces the computation time and simplifies the optimization procedure. The genetic algorithm [Manh and Lee (2014); Dong, Wei, Tian et al. (2017); Dong, Wei and Liu (2018)] is adopted for the optimization of sub-models. The optimization schedule is illustrated in Fig. 4.

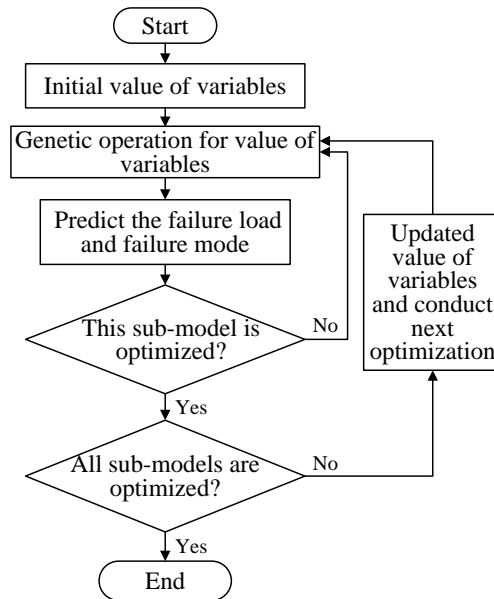


**Figure 4:** Optimization flow chart of the simplified optimization model for composite bolted joints

Step 1. Based on the initial values of the design variables (or the update values of the design variables), a genetic algorithm is used to obtain the candidate value of the variable being optimized, and the finite element model of a composite bolted joint is built to obtain an accurate stress field. Then, a modified characteristic curve method is used to predict the failure load and failure mode of the composite bolted joint.

Step 2. If the failure mode is bearing, but the sub-model has not yet been optimized according to the genetic algorithm, a new candidate value will be obtained with the genetic algorithm and Step 1 is conducted again; if the failure mode is not bearing, the candidate value is abandoned, a new candidate value will be obtained with the genetic algorithm, and Step 1 is conducted again; if this sub-model has been optimized by the genetic algorithm, the variables are updated and the next sub-model with other variables will be optimized until all the sub-models are optimal.

**4 Optimization result**

The three-step optimization strategy is applied to an ideal optimization model of a composite bolted joint, including feasible region reduction, model decoupling and one by one optimizing for the optimization of the sub-models.

#### 4.1 Initial design of the single-bolt double-lap composite joint

The initial design of the single-bolt double-lap composite joint according to the ASTM D5961 standard and the investigations described in Zhang et al. [Zhang, Zhou, Chen et al. (2016); Zhang, Liu, Zhao et al. (2014, 2015)] is listed in Tab. 2, and the laminates in the joint are made of T800 carbon/epoxy.

**Table 2:** Initial design variables of the composite single-bolt double-lap joint

Variables	Initial value	Unit	Variables	Initial value	Unit
$D$	4.76	mm	$E_{11}$	195	GPa
$e$	15	mm	$E_{22}$	8.58	GPa
$S_w$	15	mm	$G_{12}$	4.57	GPa
$t$	3.7	mm	$G_{23}$	3.15	GPa
$N$	0	N·m	$\nu_{12}$	0.33	1
$\mu$	0.4	1	$\nu_{23}$	0.49	1
$\eta$	0	mm	$X_T$	3071	MPa
$t_{ply}$	0.185	mm	$X_C$	1748	MPa
$\theta_1$	45	°	$Y_T$	88	MPa
$\theta_2$	0	°	$Y_C$	271	MPa
$\theta_3$	-45	°	$S_{12}$	143	MPa
$\theta_4$	0	°	$S_{23}$	104	MPa
$\theta_5$	90	°	$E_f$	340.46	GPa
$\theta_6$	0	°	$G_f$	47.64	GPa
$\theta_7$	45	°	$\nu_f$	0.318	1
$\theta_8$	0	°	$V_f$	0.57	1
$\theta_9$	-45	°	$E_m$	3.52	GPa
$\theta_{10}$	0	°	$G_m$	1.2	GPa
			$\nu_m$	0.35	1

#### 4.2 Reducing the feasible design region to simplify the optimization model

##### 4.2.1 Selection of dominant design variables

a) Failure load prediction with the 3D FE model and modified characteristic curve method

A parametric 3D FE model of the composite bolted joint in the ANSYS® FE code using the APDL language [Zhao, Shan, Liu et al. (2017)] was applied as shown in Fig. 5. All the components were modeled using the ANSYS® SOLID185 element. The finite element model provided stress around the hole for the modified characteristic curve method, and the latter could predict failure load and failure mode with the stress.

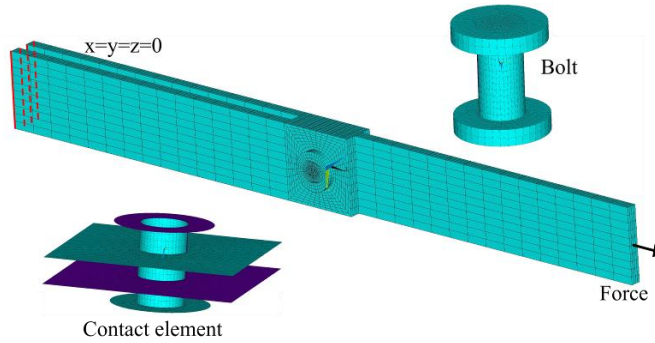


**Figure 5:** Finite element model for the stress prediction around the hole

The computational mass  $m$  of the joint is 78.4 g, and the failure load  $F$  predicted by the modified characteristic curve method is 19.08 kN, which is in good agreement with the experimental result [Camanho, Bowron and Matthews (1998)] of 20.37 kN with a relative error of -6.3%.

b) Selection of dominant variables based on the sensitivity analysis

For the single-bolt, double-lap composite bolted joint with the initial parameters presented in Tab. 2, Tab. 3 lists the actual increment  $\Delta x_i$  and the results of the sensitivity analysis  $S_i$  (Eq. (5)). Fig. 6 also illustrates the sensitivity analysis results. It follows that the  $S_i$  for the variables  $\theta_8, \theta_5, \theta_4, \nu_{23}, t, \mu, \nu_{12}, \theta_1, \theta_7, \theta_9$  and  $\theta_{10}$  are less than 0.005 kN/1. They are trivial variables for the joint failure load, while other variables are of great significance, especially the three variables  $V_f, E_f$  and  $X_C$ , which have the largest  $S_i$  and are all larger than 1 kN.

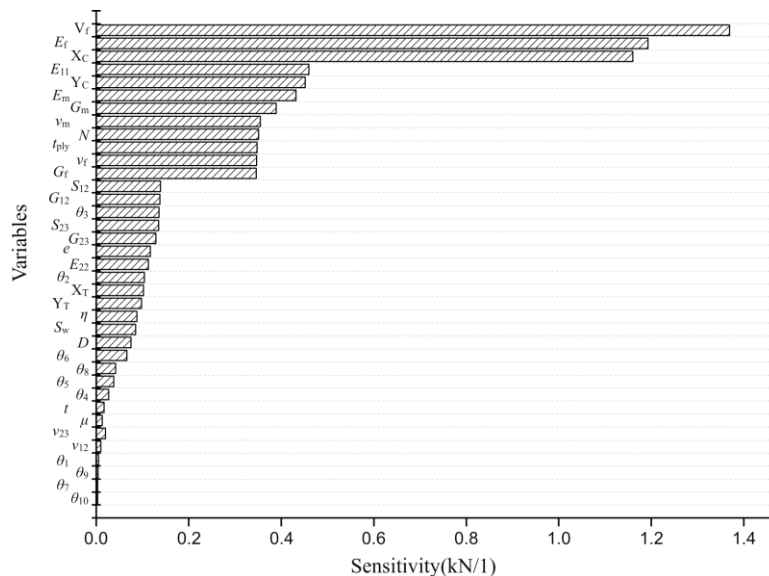


**Figure 6:** Sensitivity analysis results

It can be proven that the majority of influential variables are material parameters, such as  $V_f$ ,  $E_f$ ,  $X_C$ ,  $E_{11}$ ,  $Y_C$ ,  $E_m$ ,  $G_m$ ,  $\nu_m$ ,  $t_{ply}$ ,  $\nu_f$ ,  $G_f$ ,  $S_{12}$ ,  $G_{12}$ ,  $S_{23}$ ,  $G_{23}$ ,  $E_{22}$ ,  $X_T$ ,  $Y_T$ , and  $\eta$ . The optimization design of the composite material parameters is performed by selecting excellent material systems rather than investigating a new material system. Optimizing the material parameters described above may lead to non-existent materials; therefore, this optimization is not regarded as the optimization content of this paper. The dominant design variables ultimately include the fiber orientation  $\theta_2$ ,  $\theta_3$  and  $\theta_6$ ; geometry parameters  $e$ ,  $S_w$  and  $D$ ; and tightening torque  $N$ .

**Table 3:** Results of the sensitivity analysis of the design variables

Variables	$\Delta x$	Unit	$S$ (kN/1)	Variables	$\Delta x$	Unit	$S$ (kN/1)
$D$	0.01	mm	-0.075	$E_{11}$	3.8	GPa	0.46
$e$	0.33	mm	0.117	$E_{22}$	0.086	GPa	0.113
$S_w$	0.33	mm	0.085	$G_{12}$	0.098	GPa	0.138
$t$	0.08	mm	0.017	$G_{23}$	0.066	GPa	0.129
$N$	0.9	N·m	0.351	$\nu_{12}$	0.02	1	0.01
$\mu$	0.01	1	0.013	$\nu_{23}$	0.046	1	0.02
$\eta$	0.01	mm	-0.088	$X_T$	187.4	MPa	0.102
$t_{ply}$	0.004	mm	0.348	$X_C$	65.8	MPa	1.16
$\theta_1$	0.9	°	-0.005	$Y_T$	7.7	MPa	0.098
$\theta_2$	0.9	°	-0.104	$Y_C$	22.4	MPa	0.452
$\theta_3$	0.9	°	0.136	$S_{12}$	3.9	MPa	0.139
$\theta_4$	0.9	°	0.027	$S_{23}$	3.7	MPa	0.135
$\theta_5$	0.9	°	0.038	$E_f$	17.023	GPa	1.193
$\theta_6$	0.9	°	0.066	$G_f$	2.382	GPa	0.346
$\theta_7$	0.9	°	-0.003	$\nu_f$	0.0159	1	0.347
$\theta_8$	0.9	°	0.042	$V_f$	0.0285	1	1.369
$\theta_9$	0.9	°	0.004	$E_m$	0.176	GPa	0.432
$\theta_{10}$	0.9	°	-0.003	$G_m$	0.006	GPa	0.389
				$\nu_m$	0.0175	1	0.355

#### 4.2.2 Reducing the feasible region of dominant variables

The influence mechanisms of the three kinds of dominant variables were studied to reduce the feasible region and thus reduce the amount of optimization calculations.

##### a) Fiber orientation

The various fiber orientations and the significant stress concentration around bolt hole cause complex stress status and further lead to different failure modes. The commonly used fiber orientations in the engineering industry are  $0^\circ$ ,  $90^\circ$  and  $\pm 45^\circ$ . The relationships between different fiber orientations and the failure modes of composite bolted joints are discussed.

If  $\theta$  is  $0^\circ$ , as shown in Fig. 7, the fiber direction is parallel to the loading direction. Because of the poor matrix and fiber-matrix interface properties, the initial damage at point D is easy to propagate along the shear-out plane and leads to a sudden shear-out failure. Akatasa et al. [Akatasa and Dirikolu (2004)] and Park [Park (2001)] proved that excessive  $0^\circ$  layers in a composite bolted joint caused unexpected failure load reduction and shear-out failure mode.

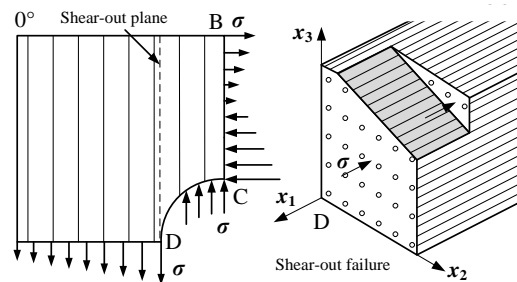


**Figure 7:** Microcosmic failure mode when fiber orientation is  $0^\circ$

If  $\theta$  is  $90^\circ$ , as shown in Fig. 8, the stress at point B is in the same direction as the fibers, so that the fibers inhibit damage initiation at point B. Because the matrix properties and fiber-matrix interface properties are too small to sustain corresponding stresses in the direction perpendicular to the fiber, interface debonding or matrix cracking occurs at both points C and D, which leads to tension failure.

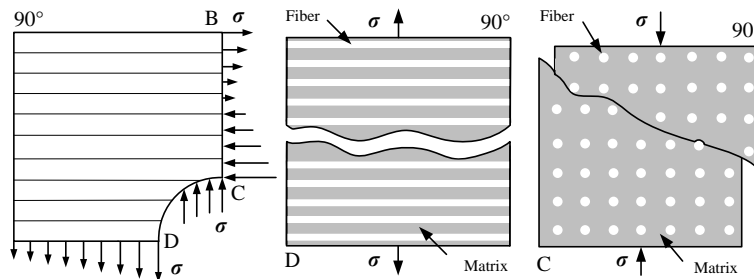


**Figure 8:** Microcosmic failure mode when fiber orientation is  $90^\circ$

If  $\theta$  is  $45^\circ$  or  $-45^\circ$ , the angles between fiber direction and stress direction at points B, C and D are all  $45^\circ$ , as shown in Fig. 9. Both compressive and tensile stress can be decomposed into the longitudinal and transverse directions of fibers, which means the fibers bear a significant degree of load at points B, C and D. Thereby, the possibility of the occurrence and propagation of damage can be reduced compared with that at the  $0^\circ$  and  $90^\circ$  layers.

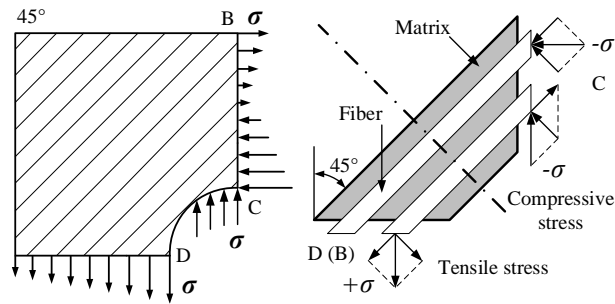


**Figure 9:** Microcosmic failure mode when fiber orientation is  $\pm 45^\circ$

The selection of the stacking sequence is important in composite bolted joint design. The reasonable proportion of the  $0^\circ$  layers contributes to increasing the failure load of composite bolted joints [Quinn and Matthews (1987)]. The  $\pm 45^\circ$  layers can reduce the stress concentration factor and avoid tension and shear-out failure mode. The  $90^\circ$  layers are able to prevent shear-out failure and maintain the transverse loading capacity. The other suggestion is that the  $0^\circ$  and  $90^\circ$  layers should not be placed at the surface, which has the largest bearing stress at point C. In addition, adjacent layers should have different fiber orientations to obtain a better interlaminar performance [Quinn and Matthews (1987); Collings (1982)]. Therefore, the constraints on the fiber orientations are  $\theta_i \neq \theta_{i+1}$  and  $10\% \leq n_{45/-45/0/90} \leq 50\%$ .

#### b) Geometry parameters

The failure behavior and joint mass are influenced by the geometric dimensions. Fig. 10 illustrates the typical stress status of the central laminate, which shows the effects of the geometric dimensions on the failure behavior of a composite joint. Those stress statuses are related to four common laminate failure modes in a composite bolted joint, namely, bearing, tensile, shear-out and cleavage [Maimi, Camanho, Mayugo et al. (2007); Camanho and Matthews (1997)].

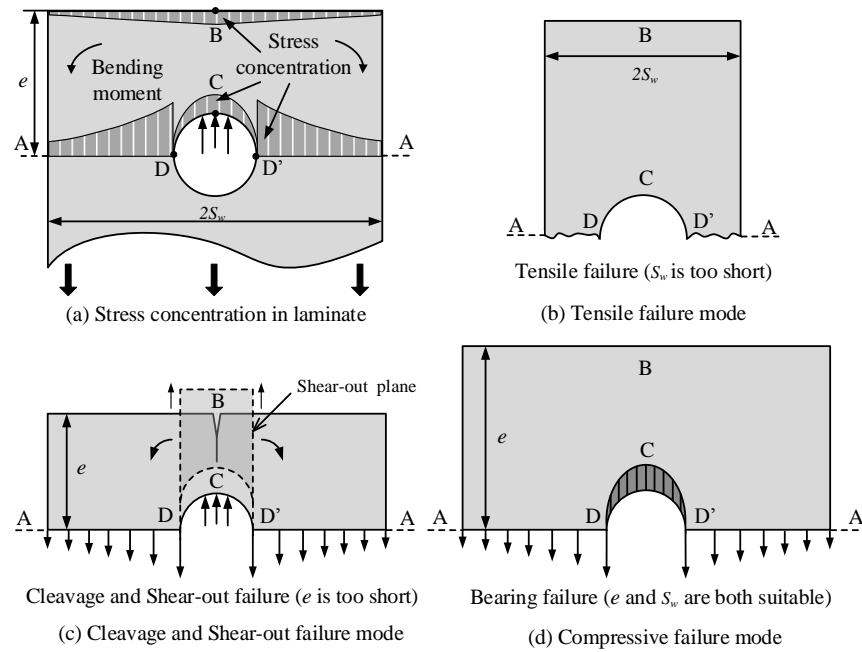


**Figure 10:** Effects of  $e$  and  $S_w$  on the failure modes of a composite bolt joint

Obviously, Section A experiences a distributed force, and a high stress concentration is exhibited at points D and D'. For the small edge distance  $S_w$ , a high stress distribution appears at section A, which directly results in a sudden tension failure, as shown in Fig. 10(b). A sufficient edge distance  $S_w$  ensures the stress at section A is low enough to avoid catastrophic tension failure. In addition, a short end distance  $e$  deteriorates the stress states at points B and D, which leads to cleavage or shear-out failure, as shown in Fig. 10(c). Therefore, the end distance  $e$  should be long enough to prevent the laminate from experiencing cleavage and shear-out failure. It is worth noting that tension, shear-out and cleavage failure always lead to catastrophic structure failure [Chang and Chang (1987); Pisano, Fuschi and Domenico (2013)]. However, the bearing damage slowly propagates near point C (Fig. 10(d)) with the increase of the external load, which provides a failure alert [Chang and Chang (1987); Guo and Nairn (2017)]. Hence, bearing failure is the expected failure mode for a composite bolted joint.

Appropriate  $e$ ,  $S_w$  and  $D$  not only contribute to increasing the failure load but also to avoiding catastrophic failure. Recent investigations have suggested that the ratios of  $e/D$  and  $S_w/D$  should be greater than 2.5 to ensure the bearing failure mode [Zhang, Liu, Zhao et al. (2015); Hart-Smith (1976)]. In addition, the upper limit of  $e$  and  $S_w$  should be restricted to decrease the composite joint mass. In the current work,  $e/D$  and  $S_w/D$ , denoted by  $\eta_e$  and  $\eta_s$ , respectively, were studied instead of  $e$  and  $S_w$ , and the optimized ranges of  $\eta_e$  and  $\eta_s$  were set as  $2.5 \leq \eta_e \leq 4$  and  $2.5 \leq \eta_s \leq 4$ .

Under an external load, the bending deformation of a bolt leads to the reduction of the contact areas between the bolt and laminates. Then, a significant stress concentration occurs

at the reduced contact areas, which deteriorates the damage status around the bolt hole and decreases the load transfer efficiency. Moreover, the thicker the central laminate, the smaller the bending deformation of the bolt, which results in a smaller stress concentration at the contact area, as shown in Fig. 11. To obtain the highest bearing load transfer efficiency, the recommended thickness of the laminate is  $1 \leq D/t \leq 2$  [Collings (1977)].

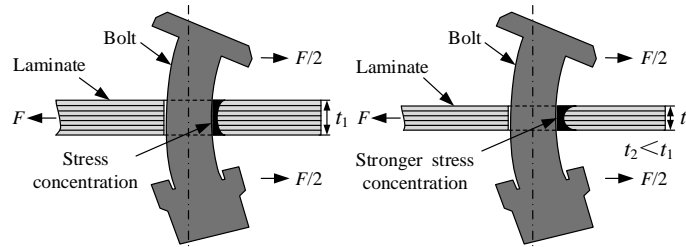


**Figure 11:** Effect of  $t$  on the failure of a composite bolted joint

c) Tightening torque

The failure load of a composite bolted joint is affected by the tightening torque  $N$ . The tightening torque causes interlaminar compression pressure around the bolt hole, which can inhibit the interlamination damage and bearing damage around the bolt hole, as shown in Fig. 12 [Sun, Chang and Qing (2002)]. The tightening torque also increases the friction force in a composite bolted joint, which contributes to the failure load improvement and prevents the adjacent layers from shear slipping [Phillips (1989); Khashaba, Sallam and Shorbagy (2006)]. Furthermore, the tightening torque provides an axial preload to the bolt, which can reduce the bending deformation of the bolt and relieve the bearing stress concentration at the outer layer of the laminate, as shown in Fig. 12(d). Thus, the tightening torque  $N$  should be included in the optimization, and the constraint is  $0 \leq N \leq 10$ .

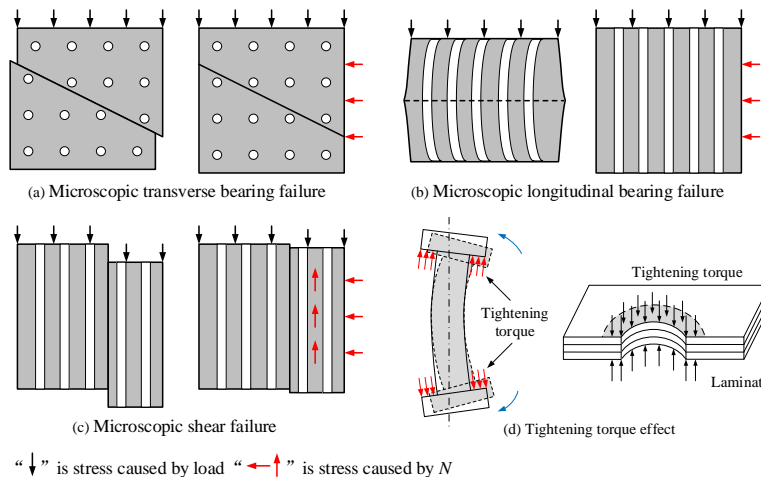


**Figure 12:** Influence of the tightening torque

**4.2.3 Simplified optimization model for composite bolted joints**

Because of the bolt bending deformation, the bolt-hole bearing stress in the outer layers is much higher than that in the inner layers. Therefore, the failure behavior of the joint is more affected by the outer layers, and the fiber orientations of the outer layers are decisive parameters of the failure behavior in the optimization design process. Thus, this paper only takes the fiber orientations of the outer five layers as optimization parameters. The final design variables in the present work are  $D$ ,  $\eta_e$ ,  $\eta_s$ ,  $N$ , and  $\theta_i$  ( $i=1, 2, 3, 4, 5$ ). The constraint conditions of the optimization variables are based on the discussion in Section 4.2.2. Consequently, the simplified optimization model for composite bolted joints can be expressed as:

$$\left\{ \begin{array}{l} \text{Minimize : } f = \frac{m(D, \eta_e, \eta_s)}{F(D, \eta_e, \eta_s, N, \theta_i)} \\ \text{Optimization variables } (x_i) : D, \eta_e, \eta_s, N, \theta_i (i = 1, 2, 3, 4, 5) \\ \text{Subject to : bearing failure mode, } n \cdot t_{ply} \leq D \leq 2n \cdot t_{ply}, 2.5 \leq \eta_e \leq 4, 2.5 \leq \eta_s \leq 4, \\ 0 \leq N \leq 10, \theta_i = \pm 45 / 0 / 90, \theta_i \neq \theta_{i+1}, (i = 1, 2, 3, 4, 5), 1 \leq n_{\pm 45/0/90} \leq 2 \end{array} \right. \quad (6)$$

where  $n$  is the total number of plies,  $n_{\pm 45/0/90}$  is the number of plies in different fiber orientations, and  $\theta$  is the fiber orientation.

**4.3 Variable decoupling**

The fiber orientation  $\theta_i$  can be decoupled from the other four variables  $D$ ,  $\eta_e$ ,  $\eta_s$ , and  $N$  because they are parameters in different levels. These four variables can be transformed in the following way:  $A=d/6$ ,  $B=\eta_e$ ,  $C=\eta_s$ , and  $D=N/5$ . With the addition of six interaction terms,  $AB, AC, AD, BC, BD$ , and  $CD$ , and four quadratic terms,  $A^2, B^2, C^2$ , and  $D^2$ , of the four variables, there are fourteen factors in total. Five levels within the constraints are set for each factor for the orthogonal experimental design. Then, the failure prediction of models under different orthogonal experiment conditions is carried out by using the method presented in Section 3.2, and variance analysis is conducted on the failure prediction results. The  $P$  value of the significance test for each factor is shown in Tab. 4.

**Table 4:**  $P$  value of the significance test for each factor

Source	Sum of Squares	df	Mean Square	$F$ value	$P$ -value
$A$	23.53	1	23.53	3433.58	< 0.0001
$B$	9.72	1	9.72	1418.98	< 0.0001
$C$	232.63	1	232.63	33946.78	< 0.0001
$D$	83.52	1	83.52	122.72	< 0.0001
$AB$	0.37	1	0.37	53.41	0.0002
$AC$	0.62	1	0.62	89.92	0.0003
$AD$	0.22	1	0.22	31.55	0.0008

$BC$	0.053	1	0.053	0.078	0.7885
$BD$	4.31	1	4.31	6.33	0.0401
$CD$	0.48	1	0.48	0.70	0.4306
$A^2$	1.38	1	1.38	201.91	< 0.0001
$B^2$	0.79	1	0.79	115.33	< 0.0001
$C^2$	0.34	1	0.34	49.30	0.0002
$D^2$	2.10	1	2.10	3.09	0.1224

From Tab. 4, it can be seen that among the factors that affect the final failure load  $F$  of the structure, the significant ones are  $A$ ,  $B$ ,  $C$ ,  $D$ ,  $A^2$  and  $B^2$ . The 6 interaction terms are of little significance, which indicates that the four macroscopic geometry variables of the joint have little influence on each other in obtaining the extreme value of the final failure load  $F$ . Therefore, the optimization model can be decoupled into five optimization sub-models; four of these sub-models are single variable optimizations with variables  $D$ ,  $e$ ,  $S_w$ , and  $N$ , and the remaining sub-model is an optimization with 5 fiber orientation variables.

Optimization sub-model (1):

$$\left\{ \begin{array}{l} \text{Minimize : } f = \frac{m(D)}{F(D)} \\ \text{Optimization variables } (x_i) : D \\ \text{Subject to : bearing failure mode, } n \cdot t_{ply} \leq D \leq 2n \cdot t_{ply} \end{array} \right. \quad (7)$$

Optimization sub-model (2):

$$\left\{ \begin{array}{l} \text{Minimize : } f = \frac{m(\eta_s)}{F(\eta_s)} \\ \text{Optimization variables } (x_i) : \eta_s \\ \text{Subject to : bearing failure mode, } 2.5 \leq \eta_s \leq 4 \end{array} \right. \quad (8)$$

Optimization sub-model (3):

$$\left\{ \begin{array}{l} \text{Minimize : } f = \frac{m(\eta_e)}{F(\eta_e)} \\ \text{Optimization variables } (x_i) : \eta_e \\ \text{Subject to : bearing failure mode, } 2.5 \leq \eta_e \leq 4 \end{array} \right. \quad (9)$$

Optimization sub-model (4):

$$\left\{ \begin{array}{l} \text{Minimize : } f = \frac{m}{F(N)} \\ \text{Optimization variables } (x_i) : N \\ \text{Subject to : bearing failure mode, } 0 \leq N \leq 10 \end{array} \right. \quad (10)$$

Optimization sub-model (5):

$$\left\{ \begin{array}{l} \text{Minimize : } f = \frac{m}{F(\theta_i)} \\ \text{Optimization variables } (x_i) : \theta_i (i = 1, 2, 3, 4, 5) \\ \text{Subject to : bearing failure mode, } \theta_i = \pm 45 / 0 / 90, \theta_i \neq \theta_{i+1}, 1 \leq n_{45/-45/0/90} \leq 2 \end{array} \right. \quad (11)$$

**4.4 Optimization based on the modified characteristic curve method**

Optimization of the five optimization sub-models for the design of the composite bolted joint is performed according to the procedure presented in Section 3.5. The optimization history is shown in Fig. 13, where the objective function values are plotted for each optimization iteration. There is only one step in optimizing the optimization sub-model (1) because the initial design value of 4.76 mm, as shown in Tab. 2, is the best choice from the available standard bolt diameters. The other four sub-models require more steps for analysis, among which the optimization sub-model (5) has the longest iteration because it includes five variables, although each variable only has four candidate values. The minimum objective function value of 3.307 in the bearing failure mode is noted.

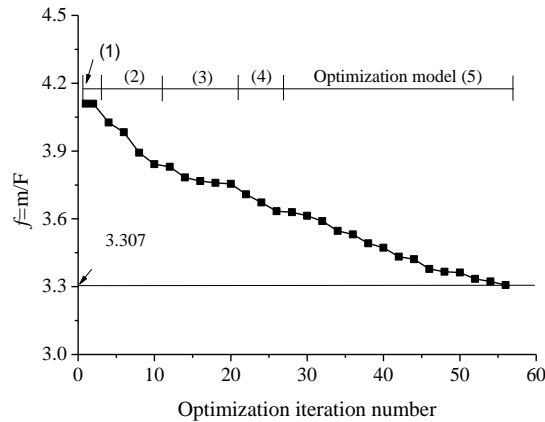


**Figure 13:** Optimization history of the composite bolted joint

The optimization design results are shown in Tab. 5 and are compared with those of the initial design. It can be seen from Tab. 5 that the bearing failure load of the optimized joint is increased by 13.5% and the mass is reduced by 8.7%. Therefore, the proposed optimization method for composite bolted joints is meaningful and effective.

**Table 5:** Optimization result and comparison to that of the initial design

Parameter	$D$ (mm)	$S_w$ (mm)	$e$ (mm)	$N$ (N·M)	$F$ (kN)	$m$ (g)	Stacking sequence	Failure mode
Initial design	4.76	15.0	15.0	4	19.08	78.4	[45/0/-45/0/90/0 /45/0/-45/0] <sub>s</sub>	Bearing
Optimization	4.76	13.8	13.8	7	21.65	71.6	[45/0/90/0/-45/0 /45/0/-45/0] <sub>s</sub>	Bearing

## 5 Conclusions

This paper presents a three-step optimization strategy based on feasible region reduction, model decoupling and the modified characteristic curve method for composite single-bolt double-lap joints. The three-step optimization strategy mainly has the following three characteristics: (1) the feasible region is reduced from two aspects to reduce the computational complexity, (2) the optimization model is decoupled into several sub-models that are easier to solve to reduce the computation cost, and (3) the modified characteristic curve method is applied for failure prediction in the optimization. An ideal optimization model for composite bolted joints is established and simplified into the optimization model with dominant design variables; then, the simplified optimization model is decoupled into 5 sub-models and solved. Comparing the result of optimization design with the result of the initial design joint, which is based on the recommendations in the ASTM D5961 standard, the final failure load of the optimized composite joint is increased by 13.5% and the mass is reduced by 8.7%. This comparison illustrates that the proposed optimization strategy is an effective method for minimizing the mass and increasing the bearing failure load of composite bolted joints.

**Acknowledgement:** This work was supported by the National Natural Science Foundation of China (11772028, 11872131, 11702012, U1864208, 11572058 and 11372020).

**Conflicts of Interest:** The authors declare that they have no conflicts of interest to report regarding the present study.

## References

- Aktasa, A.; Dirikolu, M. H.** (2004): An experimental and numerical investigation of strength characteristics of carbon-epoxy pinned-joint plates. *Composite Science and Technology*, vol. 64, no. 10-11, pp. 1605-1611.
- ASTM D 5961-13.** (2013): Standard test method for bearing response of polymer matrix composite laminates. *American Society for Testing of Material*.
- Bakar, I. A. A.; Kramer, O.; Bordas, S.; Rabczuk, T.** (2013): Optimization of elastic properties and weaving patterns of woven composites. *Composite Structures*, vol. 100, pp. 575-591.
- Camanho, P. P.; Bowron, S.; Matthews, F. L.** (1998): Failure mechanisms in bolted

CFRP. *Journal of Reinforced Plastics and Composites*, vol. 17, no. 3, pp. 205-233.

**Camanho, P. P.; Matthews, F. L.** (1997): Stress analysis and strength prediction of mechanically fastened joints in FRP: a review. *Composites Part A*, vol. 28, no. 6, pp. 529-547.

**Chang, F. K.; Chang, K. Y.** (1987): Post-failure analysis of bolted composite joints in tension or shear-out mode failure. *Journal of Composite Materials*, vol. 21, pp. 809-836.

**Coelho, P. G.; Guedes, J. M.; Rodrigues, H. C.** (2015): Multiscale topology optimization of bi-material laminated composite structures. *Composite Structures*, vol. 132, pp. 495-505.

**Collings, T. A.** (1982): On the bearing strengths of CFRP laminates. *Composites*, vol. 13, no. 3, pp. 241-252.

**Collings, T. A.** (1977): The strength of bolted joints in multi-directional CFRP laminates. *Composites*, vol. 8, no. 1, pp. 43-55.

**Dong, Y. F.; Wei, X. N.; Liu, F. R.** (2018): Novel collaborative optimization framework with a negotiation model for satellite system design. *Engineering Optimization*, vol. 50, no. 8, pp. 1395-1414.

**Dong, Y. F.; Wei, X. N.; Lu, L.; Liu, F. R.; Xu, G. D.** (2017): A novel double cluster and principal component analysis-based optimization method for the orbit design of earth observation satellites. *International Journal of Aerospace Engineering*, 6396032.

**Friedrich, S. M.; Wu, A. S.; Thostenson, E. T.; Chou, T. W.** (2011): Damage mode characterization of mechanically fastened composite joints using carbon nanotube networks. *Composites Part A*, vol. 42, no. 12, pp. 2003-2009.

**Guo, Y. J.; Nairn, J. A.** (2017): Simulation of dynamic 3D crack propagation within the material point method. *Computer Modeling in Engineering & Sciences*, vol. 113, no. 4, pp. 389-410.

**Hart-Smith, L. J.** (1976): Bolted joints in graphite-epoxy composites. *Long Beach: Douglas Aircraft Company*. Report No.: NASA-CR-144899.

**He, Y.; Aref, A. J.** (2006): An optimization design procedure for fiber reinforced polymer web-core sandwich bridge deck systems. *Composite Structures*, vol. 60, pp. 183-195.

**Khashaba, U. A.; Sallam, H. E. M.; Al-Shorbagy, A. E.** (2006): Effect of washer size and tightening torque on the performance of bolted joints in composite structures. *Composite Structures*, vol. 73, pp. 310-317.

**Kradinov, V.; Madenci, E.; Ambur, D. R.** (2007): Application of genetic algorithm for optimum design of bolted composite lap joints. *Composite Structures*, vol. 77, pp. 148-159.

**Kumar, P.; Srinivas, J.** (2018): Three phase composite cylinder assemblage model for analyzing the elastic behavior of MWCNT-reinforced polymers. *Computers, Materials & Continua*, vol. 54, no. 1, pp. 1-20.

**Li, H. S.; Gu, R. J.; Zhao, X.** (2017): Global sensitivity analysis of load distribution and displacement in multi-bolt composite joints. *Composites Part B*, vol. 116, pp. 200-210.

**Li, R.; Huong, N.; Crosky, A.; Mouritz, A. P.; Kelly, D. et al.** (2009): Improving bearing performance of composite bolted joints using z-pins. *Composite Science and*

*Technology*, vol. 69, no. 7-8, pp. 883-889.

**Lindgaard, E.; Lund, E.** (2010): Nonlinear buckling optimization of composite structures. *Computer Methods in Applied Mechanics and Engineering*, vol. 199, no. 37-40, pp. 2319-2330.

**Liu, F. R.; Lu, X. H.; Zhao, L. B.; Zhang, J. Y.; Hu, N. et al.** (2018): An interpretation of the load distributions in highly torqued single-lap composite bolted joints with bolt-hole clearances. *Composites Part B*, vol. 138, pp. 194-205.

**Maimi, P.; Camanho, P. P.; Mayugo, J. A.; Davila, C. G.** (2007): A continuum damage model for composite laminates: part I-Constitutive mode. *Mechanics of Materials*, vol. 39, no. 10, pp. 897-908.

**Manh, T. L.; Lee, J. H.** (2014): Stacking sequence optimization for maximum strengths of laminated composite plates using genetic algorithm and isogeometric analysis. *Composite Structures*, vol. 116, pp. 357-363.

**Park, H. J.** (2001): Effects of stacking sequence and clamping force on the bearing strengths of mechanically fastened joints in composite laminates. *Composite Structures*, vol. 53, pp. 213-221.

**Pelletier, J. L.; Vel, S. S.** (2006): Multi-objective optimization of fiber reinforced composite laminates for strength, stiffness and minimal mass. *Composite Structures*, vol. 84, pp. 2065-2080.

**Phillips, L. N.** (1989): *Design with Advanced Composite Materials*. Springer-Verlag Press.

**Pisano, A. A.; Fuschi, P.; Domenico, D. D.** (2013): Failure modes prediction of multi-pin joints ERP laminates by limit analysis. *Composites Part B*, vol. 46, pp. 197-206.

**Qin, T. L.; Zhao, L. B.; Xu, J. F.; Liu, F. R.; Zhang, J. Y.** (2019): Model of CEL for 3D elements in PDMs of unidirectional composite structures. *Computer Modeling in Engineering & Sciences*, vol. 118, no. 1, pp. 157-176.

**Quinn, W. J.; Matthews, F. L.** (1987): The effect of stacking sequence on the pin-bearing strength in GFRP. *Journal of Composite Materials*, vol. 11, no. 2, pp. 139-145.

**Saleeb, A. F.; Wilt, T. E.; Al-Zoubi, N. R.; Gendy, A. S.** (2003): An anisotropic viscoelastoplastic model for composites-sensitivity analysis and parameter estimation. *Composites Part B*, vol. 34, no. 1, pp. 21-39.

**Sane, A.; Padole, P. M.; Uddanwadiker, R. V.** (2018): Progressive failure evaluation of composite skin-stiffener joints using node to surface interactions and CZM. *Computer Modeling in Engineering & Sciences*, vol. 115, no. 2, pp. 281-294.

**Sun, H. T.; Chang, F. K.; Qing, X. L.** (2002): The response of composite joints with bolt-clamping loads, part II: model verification. *Journal of Composite Materials*, vol. 36, no. 1, pp. 69-92.

**Wu, J.; Burgueño, R.** (2006): An integrated approach to shape and laminate stacking sequence optimization of free-form FRP shells. *Computer Methods in Applied Mechanics and Engineering*, vol. 195, no. 33-36, pp. 4106-4123.

**Xu, G. D.; Yang, F.; Zeng, T.; Cheng, S.; Wang, Z. H.** (2016): Bending behavior of graded corrugated truss core composite sandwich beams. *Composite Structures*, vol. 138, pp. 342-351.

**Zhang, C.; Li, N.; Wang, W. Z.; Binienda, W. K.; Fang, H. B.** (2015): Progressive damage simulation of triaxial braided composite using a 3D meso-scale finite element model. *Composite Structures*, vol. 125, pp. 104-116.

**Zhang, J. Y.; Liu, F. R.; Zhao, L. B.; Fei, B. J.** (2014): A novel characteristic curve for failure prediction of multi-bolt composite joints. *Composite Structures*, vol. 108, pp. 129-136.

**Zhang, J. Y.; Liu, F. R.; Zhao, L. B.; Zhi, J.; Zhou, L. W. et al.** (2015): Influence of end distances on failure of composite bolted joints. *Journal of Reinforced Plastics and Composites*, vol. 34, no.5, pp. 388-404.

**Zhang, J. Y.; Zhou, L. W.; Chen, Y. L.; Zhao, L. B.; Fei, B. J.** (2016): A micromechanics-based degradation model for composite progressive damage analysis. *Journal of Composite Materials*, vol. 50, no. 16, pp. 2271-2287.

**Zhao, L. B.; Qin, T. L.; Zhang, J. Y.; Shan, M. J.; Fei, B. J.** (2015): Determination method of stress concentration relief factors for failure prediction of composite multi-bolt joints. *Journal of Composite Materials*, vol. 49, no. 14, pp. 1667-1680.

**Zhao, L. B.; Shan, M. J.; Liu, F. R.; Zhang, J. Y.** (2017): A probabilistic model for strength analysis of composite double-lap single-bolt joints. *Composite Structures*, vol. 161, pp. 419-427.

**Zhao, L. B.; Yang, W.; Cao, T. C.; Li, H. B.; Liu, B. R. et al.** (2018): A progressive failure analysis of all-C/SiC composite multi-bolt joints. *Composite Structures*, vol. 202, pp. 1059-1068.